Hepatic *trans*-Golgi action coordinated by the GTPase ARFRP1 is crucial for lipoprotein lipidation and assembly[S]

Deike Hesse,[1,*,†] Katrin Radloff,[*,†] Alexander Jaschke,[*,†] Merit Lagerpusch,[*,†] Bomee Chung,[*,†] Anne Tailleux,[§] Bart Staels,[§] and Annette Schürmann[1,*,†]

Department of Experimental Diabetology,* German Institute of Human Nutrition Potsdam-Rehbruecke, D-14558 Nuthetal, Germany; German Center for Diabetes Research (DZD),[†] Potsdam-Rehbruecke, Germany; and Université Lille 2,[§] Inserm U1011, Institut Pasteur de Lille, European Genomic Institut for Diabetes (EGID), FR 3508, Lille, France

Abstract The liver is a major organ in whole body lipid metabolism and malfunctioning can lead to various diseases including dyslipidemia, fatty liver disease, and type 2 diabetes. Triglycerides and cholesteryl esters are packed in the liver as very low density lipoproteins (VLDLs). Generation of these lipoproteins is initiated in the endoplasmic reticulum and further maturation likely occurs in the Golgi. ADP-ribosylation factor-related protein 1 (ARFRP1) is a small *trans*-Golgi-associated guanosine triphosphatase (GTPase) that regulates protein sorting and is required for chylomicron lipidation and assembly in the intestine. Here we show that the hepatocyte-specific deletion of *Arfrp1* (*Arfrp1*$^{liv-/-}$) results in impaired VLDL lipidation leading to reduced plasma triglyceride levels in the fasted state as well as after inhibition of lipoprotein lipase activity by Triton WR-1339. In addition, the concentration of ApoC3 that comprises 40% of protein mass of secreted VLDLs is markedly reduced in the plasma of *Arfrp1*$^{liv-/-}$ mice but accumulates in the liver accompanied by elevated triglycerides. Fractionation of *Arfrp1*$^{liv-/-}$ liver homogenates reveals more ApoB48 and a lower concentration of triglycerides in the Golgi compartments than in the corresponding fractions from control livers. In conclusion, ARFRP1 and the Golgi apparatus play an important role in lipoprotein maturation in the liver by influencing lipidation and assembly of proteins to the lipid particles.—Hesse, D., K. Radloff, A. Jaschke, M. Lagerpusch, B. Chung, A. Tailleux, B. Staels, and A. Schürmann. **Hepatic *trans*-Golgi action coordinated by the GTPase ARFRP1 is crucial for lipoprotein lipidation and assembly. *J. Lipid Res.* 2014.** 55: **41–52.**

Supplementary key words ADP-ribosylation factor-related protein 1 • very low density lipoprotein • high density lipoprotein • apolipoprotein B • apolipoprotein A1 • apolipoprotein C3 • guanosine triphosphatase

Although lipid metabolism and homeostasis have been a research focus for decades, the increasing obesity and diabetes epidemic illustrates that there is an urgent need to pin down the molecular mechanisms regulating this complex network. Furthermore, the worldwide increase in coronary heart disease caused by arteriosclerotic plaques is associated with hypertriglyceridemia (1, 2), which is also a symptom of type 2 diabetes and the metabolic syndrome. Diabetes and associated insulin resistance result in an impairment of the insulin-mediated suppression of very low density lipoprotein (VLDL) secretion in the liver and thereby in an altered lipoprotein pattern in the plasma (3). VLDL precursors are assembled in the endoplasmic reticulum (ER) and their maturation occurs in the postER compartments (4). However, how this maturation is achieved is only partially understood (4). The Golgi apparatus, as a postER compartment, is responsible for the processing and sorting of proteins, however, the contribution of specific Golgi compartments and their associated proteins for certain trafficking pathways, such as lipoprotein metabolism, is less well understood (4). To elucidate the regulatory networks that finely orchestrate these processes, further studies are needed.

ADP-ribosylation factor-related protein 1 (ARFRP1) [reviewed in (5)] is a member of the Ras super-family of small guanosine triphosphatases (GTPases) that act as molecular switches (6, 7). In the GTP-bound active state, ARFRP1 is located at the *trans*-Golgi (8) where it was shown to be involved in the targeting of certain proteins to the plasma membrane (9, 10) and to intracellular storage vesicles (10) as well as secreted proteins (11). The hepatocyte-specific deletion of *Arfrp1* results in a disturbed glucose metabolism caused by a reduced plasma membrane localization of the glucose transporter GLUT2 and a marked growth retardation partially due to a lower secretion of the

This work was supported by the German Research Foundation (DFG; SFB 958) and the German Ministry of Education and Research (BMBF: DZD, 01GI0922) and the State of Brandenburg.

Manuscript received 16 May 2013 and in revised form 14 October 2013.

Published, JLR Papers in Press, November 1, 2013
DOI 10.1194/jlr.M040089

Abbreviations: ARFRP1, ADP-ribosylation factor-related protein 1; *Arfrp1*$^{liv-/-}$, liver-specific *Arfrp1*-knockout; ER, endoplasmic reticulum; FPLC, fast-protein liquid chromatography; GTPase, guanosine triphosphatase; IHC, immunohistochemical; MTP, microsomal triglyceride-transfer protein; WB, Western blot.

[1] To whom correspondence should be addressed.
e-mail: schuermann@dife.de (A.S.); deike.hesse@dife.de (D.H.)

[S] The online version of this article (available at http://www.jlr.org) contains supplementary data in the form of three figures.

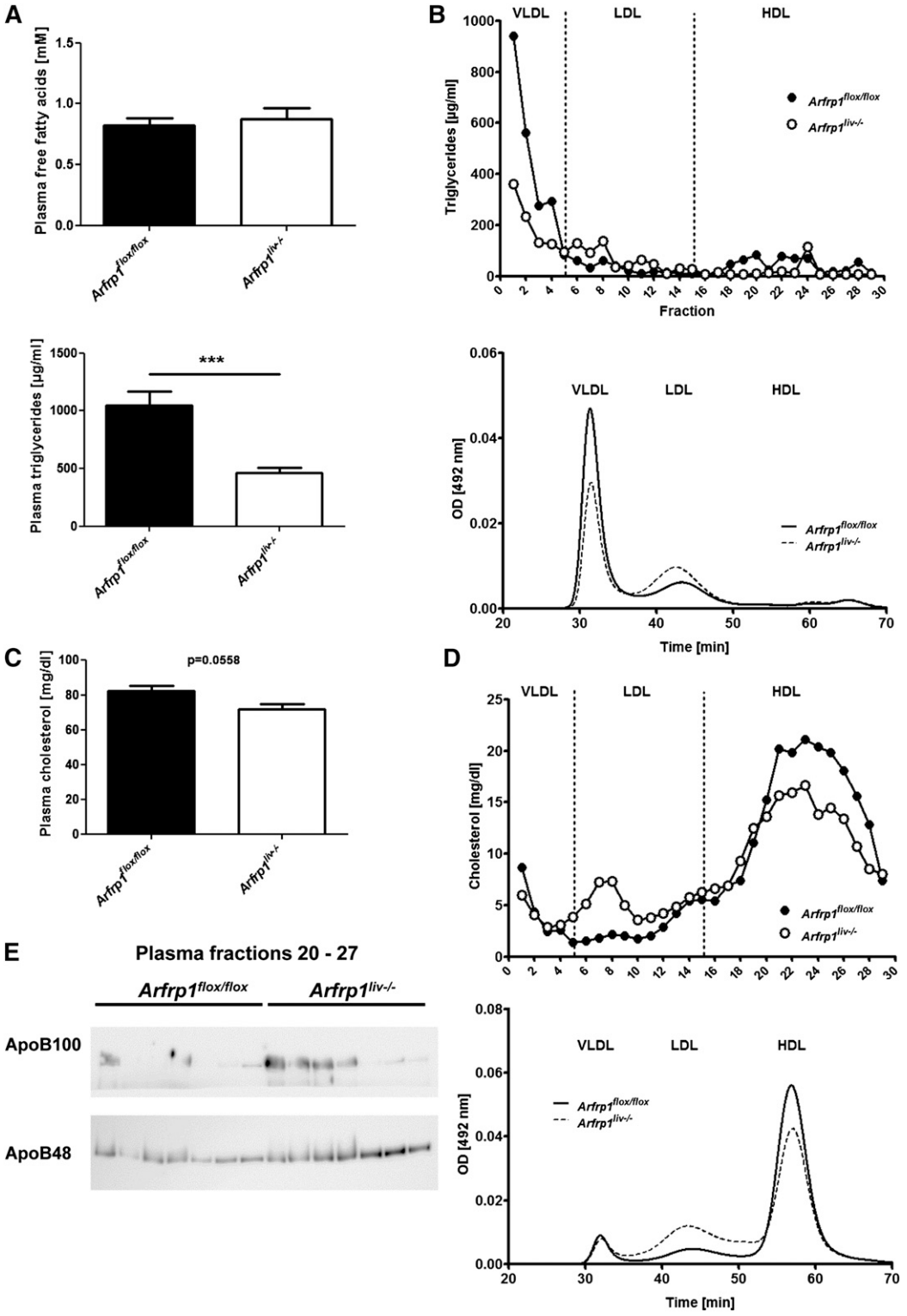

Fig. 1. Altered plasma parameters in fasted *Arfrp1*$^{liv-/-}$ mice. A: Free fatty acids (upper panel, n = 9–10) and total plasma triglyceride concentrations (lower panel, n = 19) of *Arfrp1*$^{liv-/-}$ and control mice measured after overnight fasting. B: Lower triglyceride content in VLDL plasma fractions of *Arfrp1*$^{liv-/-}$ mice after fasting determined after separation by ultracentrifugation (upper panel, pooled samples from three mice per genotype) or detected by FPLC (lower panel, n = 7–11). OD, optical density. C: Concentration of total plasma cholesterol in *Arfrp1*$^{liv-/-}$ and control mice after fasting (n = 19). D: Shift of cholesterol content from HDL-containing to LDL plasma fractions of *Arfrp1*$^{liv-/-}$ mice after fasting as determined after separation by ultracentrifugation (upper panel, pooled samples from three mice per genotype) or as detected by FPLC (lower panel, n = 7–11). E: Elevated ApoB48 and ApoB100 in *Arfrp1*$^{liv-/-}$ HDL-containing plasma fractions generated by ultracentrifugation. ***$P < 0.001$.

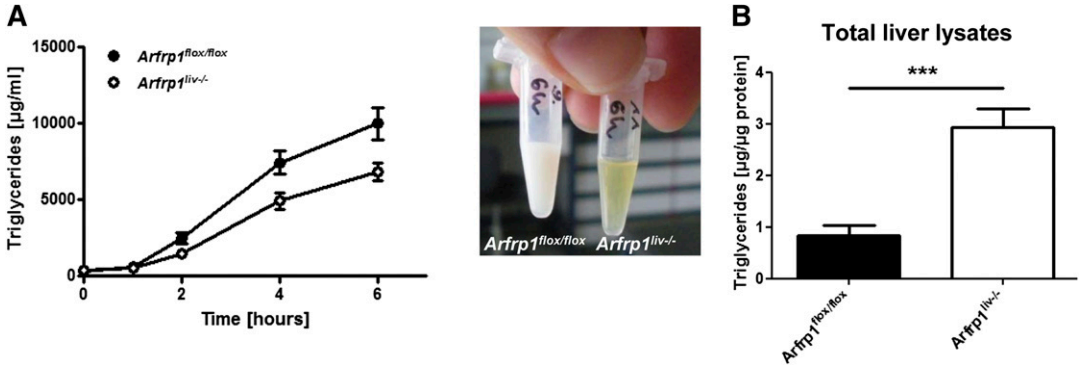

Fig. 2. Inhibition of lipoprotein lipase after fasting resulted in reduced VLDL secretion in *Arfrp1*$^{liv-/-}$ mice. A: Intraperitoneal application of Triton WR-1339 led to lower triglyceride levels in *Arfrp1*$^{liv-/-}$ mice determined by colorimetric assay and visual inspection after 6 h (n = 15–16). B: Liver triglycerides were elevated in *Arfrp1*$^{liv-/-}$ mice after fasting and consecutive Triton WR-1339 treatment (n = 8–9). ***$P < 0.001$.

insulin-like growth factor IGF1 from hepatocytes (11). A lipodystrophic phenotype was initiated by a fat cell-specific deletion of *Arfrp1*. Diminished lipid droplet fusion and elevated lipolysis were responsible for smaller lipid droplets in brown adipose tissue (12). Furthermore, in a recent study it was shown that in the intestine ARFRP1 is involved in the formation and lipidation of lipid-carrying chylomicrons (13). Besides its fundamental role in whole body glucose homeostasis, the liver is further essential for the distribution of lipids in the body via synthesis and secretion of VLDLs. Because the organization of VLDLs is very similar to that of chylomicrons, the aim of this study was to clarify the impact of the GTPase ARFRP1 and the *trans*-Golgi for lipoprotein assembly and release in the liver.

MATERIALS AND METHODS

Liver-specific *Arfrp1*-knockout (*Arfrp1*$^{liv-/-}$) mice were generated as described (11) and compared with their control littermates (*Arfrp1*$^{flox/flox}$). All experiments were performed at the age of 5 weeks because of an incomplete suppression of *Arfrp1* expression at later time points. The animals were housed in a controlled environment (20 ± 2°C, 12/12 h light/dark cycle) and had free access to water and standard diet (V153x, Ssniff, Soest, Germany). For fasting conditions, diet was deprived overnight. All animal experiments were approved by the ethics committee of the State Agency of Environment, Health, and Consumer Protection (State of Brandenburg, Germany).

Determination of ApoC3, free fatty acids, triglycerides, and cholesterol in plasma and liver samples of fasted mice

For the quantification of ApoC3 in plasma and liver samples (25 µg) a rat/mouse ELISA was used and applied according to the manufacturer's instructions (Apc3, Abnova, Germany). Nonesterified free fatty acid, triglyceride, and cholesterol content of plasma was determined as described (14). Plasma cholesterol was determined by enzymatic colorimetric assay (Cholesterol liquicolor; Human, Wiesbaden, Germany).

For the quantitative determination of triglyceride content from murine livers (15), livers were homogenized in 10 mM sodium dihydrogen phosphate, 1 mM EDTA, and 1% polyoxyethylene(10) tridecyl ether; incubated for 5 min at 37°C; and the triglycerides in the supernatant were detected with a commercial kit (Randox-TR-210, Crumlin, UK).

Lipid distribution in the lipoprotein fractions

To obtain lipoprotein fractions for fast-protein liquid chromatography (FPLC) analysis, each individual plasma sample was loaded on a filtration chromatography column onto a Superose 6 10/300 GL column (GE Healthcare), which separates lipoproteins according to their size, and cholesterol and triglyceride concentrations were continuously measured in the effluent using an enzymatic assay at an optical density of 492 nm as described (16–18). This system allows separation of the three major lipoprotein classes; VLDLs, LDLs, and HDLs. Cholesterol or triglyceride concentrations were determined in the eluted fractions. Accumulated data were analyzed by the Millenium 20/0 program (Waters).

The area under each peak is proportional to the lipid concentration in the respective lipoprotein fraction. Results are expressed as lipid concentration in VLDLs, LDLs, and HDLs as previously described (16). Moreover, data are also presented as cholesterol- and triglyceride-mean profiles obtained with each individual plasma sample of each group.

Determination of hepatic VLDL secretion

To determine maximum hepatic VLDL secretion, basal blood samples were collected from the tail vein after fasting overnight. Triton WR-1339 (15% in saline, 0.5 g/kg) was injected intraperitoneally to block lipoprotein lipase and blood was sampled 1, 2, 4, and 6 h after application. After centrifugation, total triglyceride content was determined using a serum triglyceride determination kit (TR0100, Sigma, USA).

To investigate VLDL composition, mice were fasted overnight and blood samples were subjected to fractionation (350,000 *g*, 4 h, 16°C; OptiPrep, Axis-Shield, UK) in order to separate different lipoprotein fractions. Subsequently, triglyceride and cholesterol content of fractions were determined and apolipoprotein distribution was assessed by Western blotting.

Detection of ApoB48/100 synthesis and clearance by pulse-chase experiments

Primary hepatocytes were isolated from 12-week-old mice and *Arfrp1* expression was suppressed by siRNA as described (11). To determine ApoB48/100 synthesis and degradation in primary hepatocytes, intracellular pools of cysteine and methionine were depleted by incubation with Cys-free and Met-free DMEM for 30 min prior to labeling with [35S] Promix (100 µCi/500 µl) for 2 h (19). For chase experiments cells were consecutively incubated with normal DMEM for 3 h. Immunoprecipitation of ApoB48/100

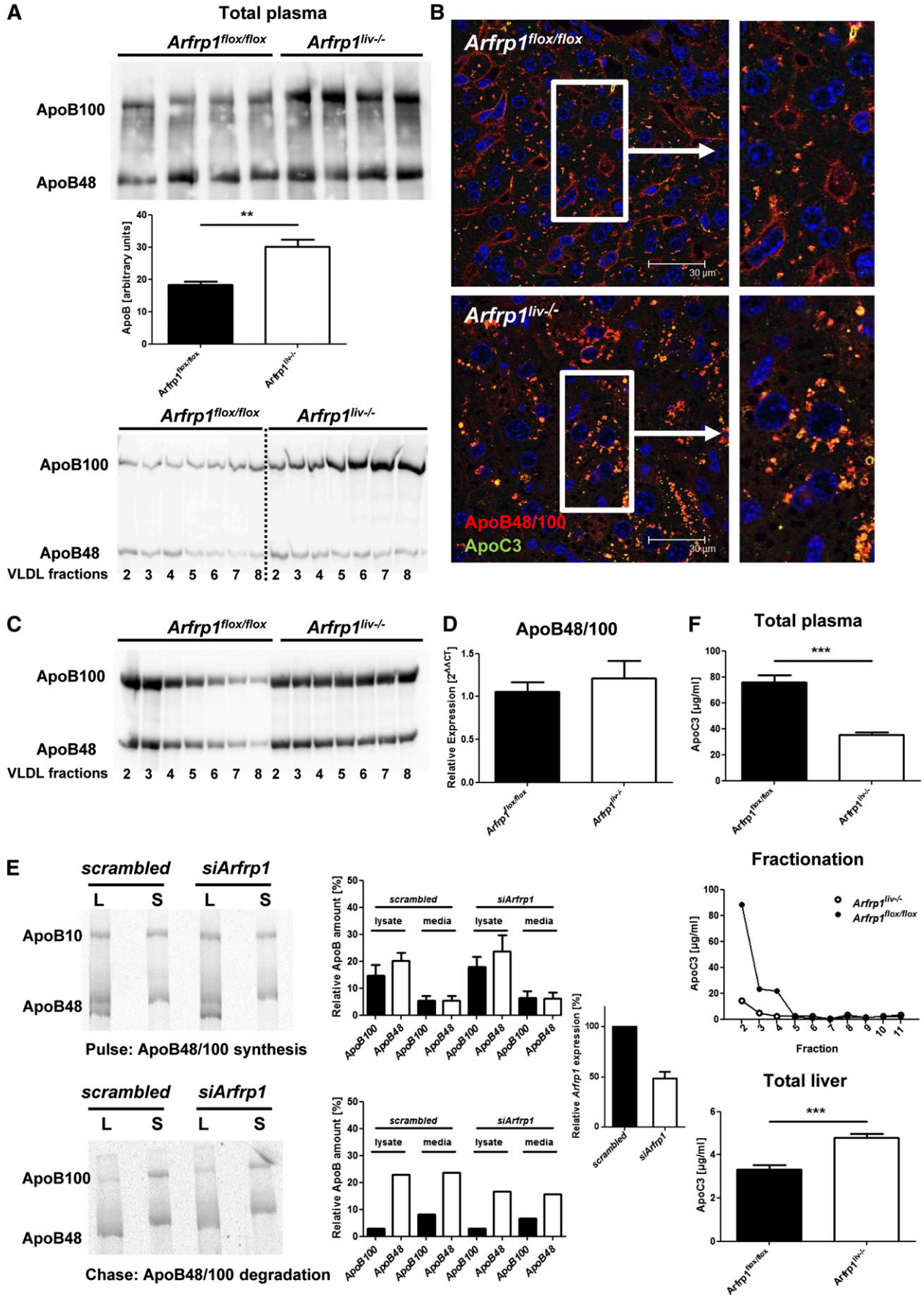

Fig. 3. Detection of apolipoproteins in the plasma and liver of control and *Arfrp1*$^{liv-/-}$ mice. A: Elevated plasma concentration of ApoB48/100 in *Arfrp1*$^{liv-/-}$ mice after fasting as determined by WB (left, upper panel) and immunonephelometric assay (left, middle

from cell lysates and cultured media/supernatant was carried out, separated on a 6% gel which was dried prior to visualization on a phosphor imager system (Storm 820, Molecular Dynamics). Band intensity was quantified by Image Quant 5.2 (Molecular Dynamics).

Triglyceride synthesis in primary hepatocytes

To determine the rate of de novo triglyceride synthesis, primary hepatocytes were transfected with scrambled siRNA or *siArfrp1* and then incubated with [^{14}C]-labeled glucose (1 μCi/ml) overnight (20). Triglycerides from cells were isolated by chloroform-methanol extraction and the addition of $CaCl_2$ to prevent contamination of the aqueous phase with lipids. Lipid extracts were dried and redissolved in chloroform prior to counting in a scintillation counter (LS6000LL; Beckman Coulter, Krefeld, Germany).

Subcellular fractionation of liver homogenates

Livers of fasted *Arfrp1*$^{liv-/-}$ and control mice were minced in homogenization buffer [0.25 M sucrose, 1 mM EDTA, 20 mM HEPES KOH (pH 7.4), and protease inhibitor], homogenized by a potter, and filtered through gauze (70 μm). After removing the nuclei by centrifuging at 1,500 *g* for 10 min at 4°C, the homogenate was separated by Optiprep density gradient centrifugation according to the manufacturer's instructions (Axis-Shield, UK). The gradient was collected in fractions of 1 ml at the end of the centrifugation. Aliquots were used to determine triglyceride concentration in fractions (Serum Triglyceride Determination kit, Sigma, Germany). Proteins in the fractions were concentrated using trichloroacetic acid to be analyzed by Western blotting (13).

Microsomal triglyceride transfer protein activity assay

The activity of microsomal triglyceride transfer protein (MTP) was determined as described in Jaschke et al. (13). Liver tissues were homogenized and 100 μg of protein were used for the assay.

Quantitative real-time PCR, Western blot, and immunohistochemical analysis

The methods were performed as described (11). The following gene expression assays were used: *Eef2* (Mm01171434_g1), *Apob* (Mm01545159_m1), *Dgat2* (Mm00499530_m1), and *Fasn* (Mm00662319_m1) (all from Applied Biosystems, Darmstadt, Germany). For protein detection the following primary antibodies were used: PLIN2 [Western blot (WB), 1:1,000; immunohistochemistry (IHC), 1:500 (Progen Biotechnik, Heidelberg, Germany)]; ApoA1 [WB, 1:2,000 (Abcam, Cambridge, UK)]; ApoB48/100 [WB, 1:1,000; IHC, 1:500 (Meridian Life Science, Memphis, TN)]; ApoC3 [IHC, 1:100 (Abcam)]; carboxylesterase 1/esterase-x [WB, 1:1,000 (Abcam)]; MTP [WB, 1:1,000 (Abcam)]; calnexin [WB, 1:2,000 (Abcam)]; syntaxin-6 [WB, 1:2,000 (BD Bioscience, Heidelberg, Germany)]; p115 [WB, 1:2,000 (BD Bioscience)]; and ARFRP1 (11). Secondary antibodies were labeled with horse-radish peroxidase or with immunofluorescent dyes for visualization on a confocal microscope (Leica-TCS-SP2; Microsystems, Heidelberg, Germany).

Furthermore, ApoA1 and ApoB48/100 were measured by immunonephelometric assays using specific mouse antibodies developed in rabbits as previously described (21).

Histological staining of intracellular lipids

To visualize stored triglycerides in liver sections, Oil-Red O staining was utilized. Therefore, microscopic slides were air dried, fixed in 4% formaldehyde, and washed in 60% isopropyl alcohol. Staining was performed for 10 min in Oil-Red O solution (0.3% Oil-Red O in 60% isopropyl alcohol) and thereafter slides were rinsed in 60% isopropyl alcohol before nuclei were counterstained with hematoxylin. The morphometric measurement of lipid droplets was performed using a Keyence BZ-9000 microscope for picture acquisition and the corresponding software for quantification (Neu-Isenburg, Germany).

Data analysis

Statistical differences were determined by nonparametric Mann-Whitney-Wilcoxon test with significance levels set at $P < 0.05$ (*), $P < 0.01$ (**), and $P < 0.001$ (***). Data are presented as means ± standard error of the mean (SEM). For statistical analysis and for graphical presentation GraphPad Prism (5.0; GraphPad Software, San Diego, CA) was used.

RESULTS

Reduced hepatic triglyceride release in *Arfrp1*$^{liv-/-}$ mice

VLDLs are the main cargo of triglycerides released by the liver under fasting conditions. To investigate the synthesis and release of VLDLs from the liver, mice expressing or lacking ARFRP1 in the liver were exposed to an overnight fasting period and plasma triglycerides and apolipoproteins were investigated. The amount of free fatty acids in the plasma of *Arfrp1*$^{liv-/-}$ and control mice was not different (**Fig. 1A**), however, plasma triglycerides of *Arfrp1*$^{liv-/-}$ mice were significantly lower compared with the control animals (Fig. 1A). This difference in plasma triglycerides was mainly due to a lower amount of triglycerides in the VLDL fraction of the plasma of *Arfrp1*$^{liv-/-}$ mice [density < 1.006 g/ml in Optiprep (22)] (Fig. 1B) visible by the quantification of triglycerides after fractionation by ultracentrifugation (Fig. 1B, upper panel) as well as by FPLC (Fig. 1B, lower panel). The VLDL fraction of *Arfrp1*$^{liv-/-}$ mice contained fewer triglycerides (*Arfrp1*$^{flox/flox}$, 31.1 ± 3.7 mg/dl; *Arfrp1*$^{liv-/-}$, 19.6 ± 2.3 mg/dl; $P < 0.05$), whereas more triglycerides were found in the LDL fraction (density 1.01–1.030 g/ml; *Arfrp1*$^{flox/flox}$, 11.8 ± 1.0 mg/dl; *Arfrp1*$^{liv-/-}$, 17.1 ± 1.3 mg/dl; $P < 0.05$).

panel; n = 6–10). WB of ApoB48/100 after fractionation of plasma by ultracentrifugation indicates increased ApoB100 in VLDL fractions of *Arfrp1*$^{liv-/-}$ plasma (left, lower panel). B: Immunohistochemical costaining of ApoB48/100 and ApoC3 on liver sections of *Arfrp1*$^{liv-/-}$ and control mice. C: Increased ApoB48 and ApoB100 in VLDL plasma fractions of *Arfrp1*$^{liv-/-}$ mice after inhibition of LPL by Triton WR-1339. D: Unaltered *Apob* mRNA in livers of *Arfrp1*$^{liv-/-}$ and control mice as determined by quantitative real-time PCR. E: Inhibition of *Arfrp1* expression in primary hepatocytes (right panel) results in no alterations in ApoB48/100 synthesis (upper panel) or intracellular degradation (lower panel) in pulse-chase experiments. L, lysate; S, cultured media/supernatant. F: Reduced ApoC3 in total plasma of *Arfrp1*$^{liv-/-}$ mice as determined by ELISA (upper panel, n = 8). ELISA of ApoC3 after fractionation of plasma by ultracentrifugation indicated reduced ApoC3 levels in VLDL fractions of *Arfrp1*$^{liv-/-}$ mice (middle panel). **$P < 0.01$, ***$P < 0.001$.

This observation indicated that the lack of ARFRP1 alters lipid distribution in the different plasma lipoprotein fractions. Accordingly, fractions 16–30 (density > 1.030 g/ml) from *Arfrp1*$^{liv-/-}$ plasma that are supposed to contain HDLs are a mixture of smaller VLDLs plus true HDLs that exhibit not only lower triglycerides (Fig. 1B) but also lower cholesterol concentrations (Fig. 1D; *Arfrp1*$^{flox/flox}$, 63.1.1 ± 2.3 mg/dl; *Arfrp1*$^{liv-/-}$, 50.9 ± 2.6 mg/dl; $P < 0.01$). This resulted in a tendency of total plasma cholesterol to be reduced in *Arfrp1*$^{liv-/-}$ mice (Fig. 1C). In addition, ApoB48/100 content in the HDL-containing plasma fractions of *Arfrp1*$^{liv-/-}$ mice was slightly elevated (Fig. 1E).

A reduced plasma triglyceride accumulation in *Arfrp1*$^{liv-/-}$ mice was accentuated by the application of the lipoprotein lipase inhibitor Triton WR-1339 after fasting, which allows determination of triglyceride release by the liver. In control mice, a strong increase of plasma triglycerides indicated an accumulation of VLDL particles in the plasma (**Fig. 2A**). In comparison, only a slight increase in triglycerides was observed in the plasma of *Arfrp1*$^{liv-/-}$ mice. As a consequence, hepatic triglycerides revealed elevated lipid levels in *Arfrp1*$^{liv-/-}$ mice compared with control livers (Fig. 2B).

Altered secretion of VLDL-associated apolipoproteins in *Arfrp1*$^{liv-/-}$ mice

ApoB48/100, as the main structural lipoprotein in VLDLs, was elevated in the plasma of *Arfrp1*$^{liv-/-}$ mice as determined by WB analysis and immunonephelometric assay (**Fig. 3A**, upper and middle panel). In addition, plasma fractionation after ultracentrifugation and consecutive WB analysis of the VLDL fraction indicated an accumulation of ApoB48/100 in VLDL particles (Fig. 3A, lower panel). Furthermore, immunohistochemical analyses of liver sections revealed an intracellular accumulation of ApoB48/100 in *Arfrp1*$^{liv-/-}$ livers (Fig. 3B). A similar increase of ApoB100 was determined in the VLDL fraction from *Arfrp1*$^{liv-/-}$ mice after Triton WR-1335 treatment (Fig. 3C). In order to test whether ARFRP1 influences ApoB48/100 synthesis, we measured mRNA of *Apob* by quantitative real-time PCR without detecting differences between the genotypes (Fig. 3D). For studying the ApoB48/100 protein synthesis and clearance, we isolated hepatocytes from 12-week-old C57BL/6 mice, suppressed *Arfrp1* expression by transfecting siRNA, and performed a pulse-chase experiment. The amount of ApoB48/100 immunoprecipitated from the lysates and from the supernatant was unaltered after depletion of *Arfrp1* 2 h after treatment with ^{35}S-labeled amino acids (Fig. 3E, upper panel). The stability of ApoB48/100 was unaffected in *siArfrp1* hepatocytes compared with control transfected cells (Fig. 3E, lower panel).

Besides ApoB48/100, other apolipoproteins such as ApoC3, which with 40% of protein mass in secreted VLDLs represents a major apoprotein in these lipoproteins (23), are synthesized by the liver and attached to VLDLs prior to secretion. In the plasma of fasted *Arfrp1*$^{liv-/-}$ mice, ApoC3, that acts as an inhibitor of plasma lipoprotein lipase (24), was significantly less abundant than in *Arfrp1*$^{flox/flox}$ mice (Fig. 3F, upper panel). This difference was most obvious in the VLDL-containing plasma part after fractionation by ultracentrifugation (Fig. 3F, middle panel). However, ApoC3 appeared to accumulate in liver extracts of *Arfrp1*$^{liv-/-}$ mice because the levels were significantly higher in total liver extracts of these mice (Fig. 3F, lower panel). Nevertheless, the mRNA of *Apoc3* was unaltered (data not shown). IHC analysis of livers indicated an intracellular accumulation of ApoC3 in *Arfrp1*$^{liv-/-}$ mice which was colocalized with ApoB48/100 (Fig. 3B).

Because ARFRP1 is known to act at the *trans*-Golgi (8), we next isolated intracellular fractions (ER and Golgi compartments) from liver homogenates of *Arfrp1*$^{flox/flox}$ and *Arfrp1*$^{liv-/-}$ mice by gradient centrifugation and detected the apoprotein and triglyceride concentrations. As expected, ARFRP1 associated with the *trans*-Golgi fractions that were syntaxin-6 positive (**Fig. 4A**). In the ER (positive for calnexin), levels of ApoB48 were not different between the genotypes. However, in the Golgi fractions (*trans*- as well as *cis/median*-Golgi) of *Arfrp1*$^{liv-/-}$ livers, we detected more ApoB48 than in the corresponding fractions from *Arfrp1*$^{flox/flox}$ livers (Fig. 4B). Comparing ApoB48 levels of all fractions from *Arfrp1*$^{flox/flox}$ and *Arfrp1*$^{liv-/-}$ livers, it appears that the latter contain more ApoB48 (supplementary Fig. III). Measurement of the triglycerides in the intracellular fractions showed only moderate differences. In samples of *Arfrp1*$^{liv-/-}$ liver the triglyceride concentrations were higher in the *cis/median*-Golgi (positive for p115) but lower in the ER fractions, whereas the *trans*-Golgi fractions exhibited similarly low levels in both genotypes (Fig. 4C).

Reduced hepatic release of the HDL-associated ApoA1 in *Arfrp1*$^{liv-/-}$ mice

ApoA1, as the major protein component of HDLs, is synthesized in the liver and the intestine (25). The amount of ApoA1 in the plasma of *Arfrp1*$^{liv-/-}$ mice was reduced as determined by WB and immunonephelometric assay (**Fig. 5**, upper and middle panels). However, *Apoa1* mRNA was unaltered between genotypes (data not shown), whereas total ApoA1 was markedly reduced in *Arfrp1*$^{liv-/-}$ liver lysates (Fig. 5, lower panel)

Accumulation of lipids and altered lipid storage in *Arfrp1*$^{liv-/-}$ livers after fasting

The isolation of triglycerides from the livers of fasted mice revealed a higher triglyceride concentration in *Arfrp1*$^{liv-/-}$ mice (**Fig. 6B**), which was also obvious after Oil-Red O staining of liver sections (Fig. 6A). This elevated lipid storage in *Arfrp1*$^{liv-/-}$ livers was accompanied by an increased hepatic expression of PLIN2 and localization of PLIN2 to the lipid droplets (supplementary Fig. I). Furthermore, these stainings indicated an alteration in lipid droplet size between the genotypes, whereas the total number of lipid droplets was unchanged between genotypes (Fig. 6C). Morphometric analysis of lipid droplet size in liver sections of fasted *Arfrp1*$^{liv-/-}$ and control mice indicated a trend toward larger lipid droplets in *Arfrp1*$^{liv-/-}$ livers (Fig. 6D).

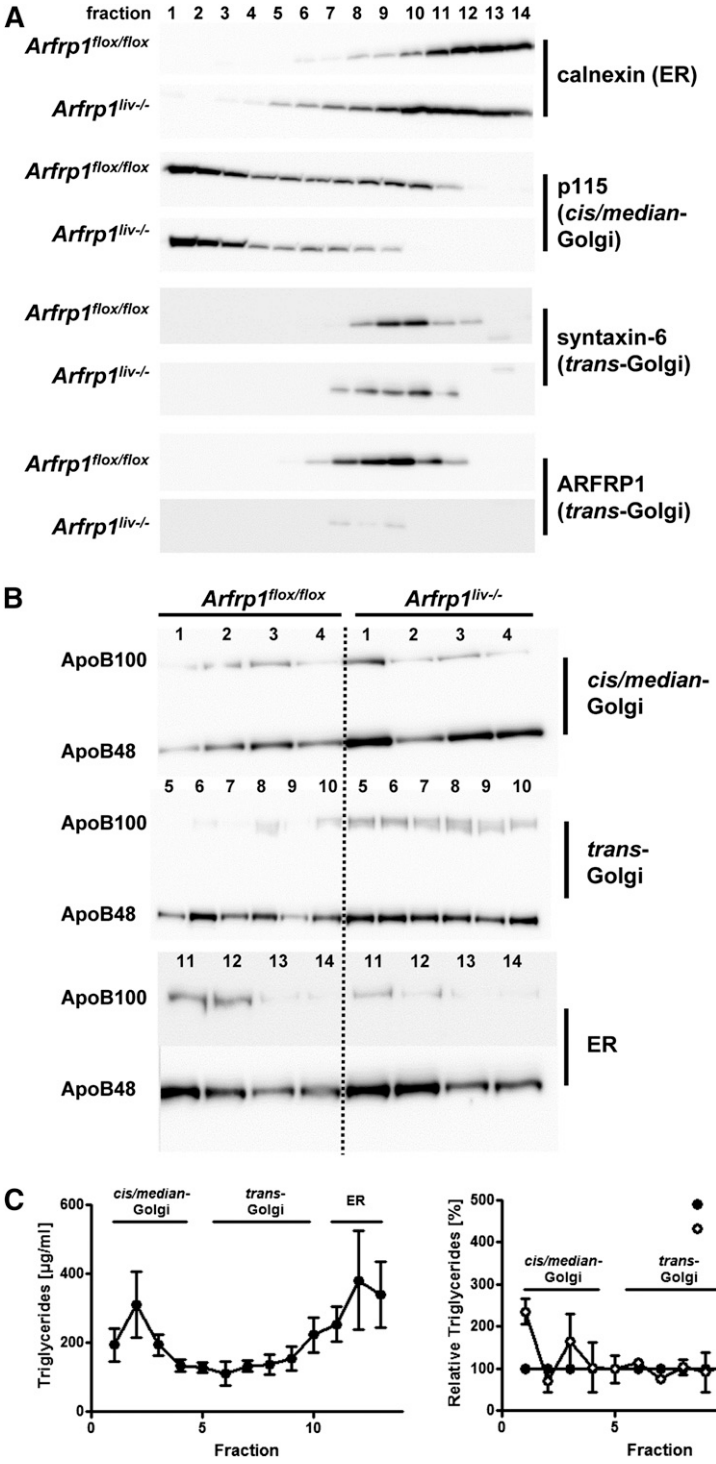

Fig. 4. Subcellular fractionation for Golgi and ER compartments of liver homogenates. A: Identification of ER and Golgi compartments by WB for marker proteins. B: Increased amount of ApoB48 and ApoB100 in *Arfrp1*$^{liv-/-}$ Golgi fractions. C: Triglyceride distribution in ER and Golgi fractions of control livers (left panel) and relative triglyceride content in *Arfrp1*$^{liv-/-}$ fractions with control values set as 100% (right panel). *Cis/median*-Golgi fractions of *Arfrp1*$^{liv-/-}$ livers contained slightly more triglycerides, whereas triglycerides in ER fractions were reduced.

Hepatic lipid synthesis and VLDL lipidation in the ER in *Arfrp1*$^{flox/flox}$ and *Arfrp1*$^{liv-/-}$ mice

In order to test whether ARFRP1 influences the hepatic triglyceride synthesis before the lipids are incorporated into VLDL particles, we treated isolated hepatocytes transfected with scrambled or *Arfrp1*-specific siRNA with ^{14}C-glucose, isolated the lipids, and determined ^{14}C incorporated into triglycerides. As shown in **Fig. 7B**, triglyceride synthesis was not different between control and *Arfrp1*-depleted hepatocytes. We furthermore studied the expression of enzymes involved in triglyceride synthesis by quantitative real-time PCR. DGAT2 catalyzes the reesterification of

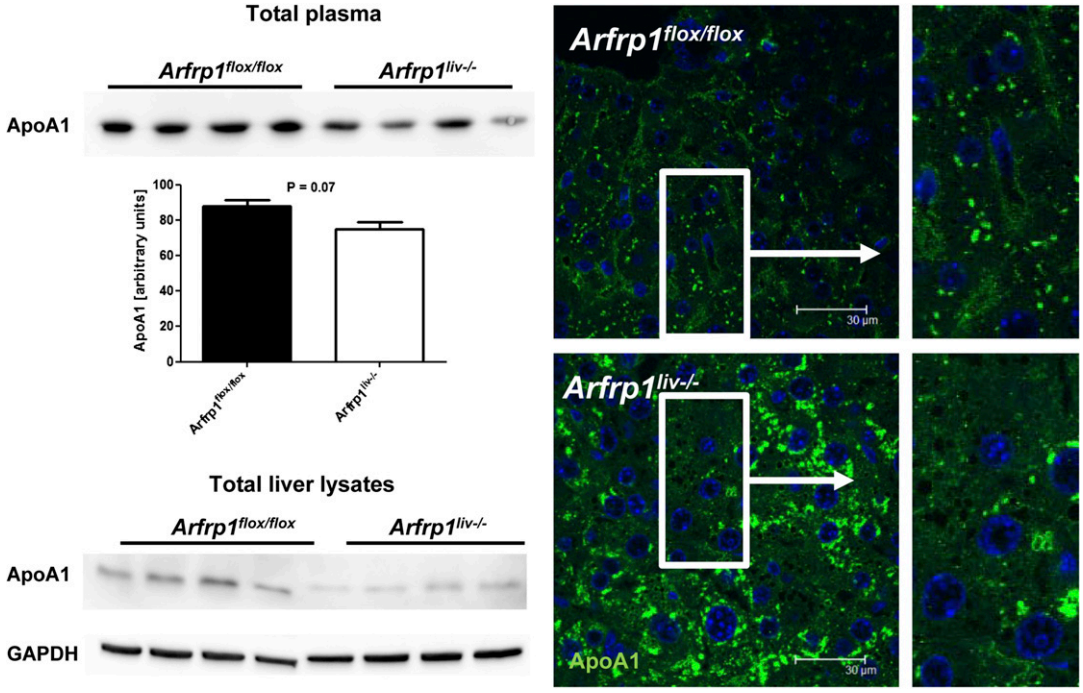

Fig. 5. Detection of ApoA1 in the plasma and livers of control and *Arfrp1*$^{liv-/-}$ mice. Decreased plasma concentration of ApoA1 in *Arfrp1*$^{liv-/-}$ mice after fasting as determined by WB (upper left panel) and immunonephelometric assay (middle left panel, n = 6–11). WB of ApoA1 of *Arfrp1*$^{liv-/-}$ liver lysates indicates reduced ApoA1 compared with control livers (lower left panel). Immunohistochemical staining of ApoA1 on liver sections of *Arfrp1*$^{liv-/-}$ and control mice (right panel).

triglycerides (26) and its mRNA was significantly lower in livers from *Arfrp1*$^{liv-/-}$ mice (Fig. 7A, upper panel). De novo fatty acid synthesis appeared to be unaltered, as there was no genotype-specific difference in the amount of *Fasn* mRNA (27) (Fig. 7A, lower panel). The initial lipidation of preVLDL particles involves the transfer of triglycerides onto ApoB48/100 particles at the ER and is facilitated by MTP (28). The measurement of MTP protein revealed no alterations in total liver lysates (supplementary Fig. IIA, upper panel) and in the Golgi and ER fractions between the genotypes (supplementary Fig. IIB). In addition, the activity of MTP in liver lysates of fasted mice indicated no influence of the deletion of hepatic *Arfrp1* on transfer of triglycerides to preVLDL particles in the ER (supplementary Fig. IIA, lower panel). Furthermore, initial lipidation of preVLDLs can occur by lipolysis of intracellular lipid droplets. The hepatic hydrolase carboxylesterase 1/esterase-x mediates this step and knockout mice exhibit an elevated VLDL secretion and fatty liver (29). However, the total amount of carboxylesterase 1 in liver lysates was unaltered between the genotypes (supplementary Fig. IIC).

DISCUSSION

The liver plays a central role for an optimal lipid distribution in the whole body. By specifically deleting the GTPase ARFRP1 in hepatocytes, the impact of *trans*-Golgi action on the VLDL lipidation as well as on the assembly of apoproteins to the VLDL particles was demonstrated. In the absence of ARFRP1, the triglyceride content of VLDL was markedly reduced, associated with a striking reduction of ApoC3 concentration in plasma and an accumulation of VLDL particles in the Golgi. As a consequence, the lipid content and ApoC3 levels within the liver were higher in the absence of ARFRP1.

Under fasting conditions, the liver is highly important for the redistribution of lipids delivered from adipose tissue after lipolysis to peripheral organs by synthesis and secretion of VLDLs. VLDL assembly is initiated in the ER and particles are thought to be further lipidated and modified in the Golgi (3). To avoid premature degradation of newly synthesized ApoB48/100, initial lipidation by MTP occurs in the ER and produces lipid-poor VLDL particles, also designated as VLDL2 (28), whereas unlipidated ApoB48/100 is directly degraded (28). However, MTP appears not to be required for final bulk lipidation of VLDL particles (30). As the amount, the distribution, and the activity of MTP as well as ApoB48/100 expression were not reduced in *Arfrp1*$^{liv-/-}$ livers, initial synthesis and lipidation of VLDL2 appeared unaffected. However, elevated plasma levels of ApoB100 and reduced triglycerides in the VLDL fraction of *Arfrp1*$^{liv-/-}$ mice could indicate a premature release of VLDL2. ApoC3 was described to directly interact with lipids via its helix 5, thereby facilitating triglyceride incorporation into VLDLs independently of MTP activity (31). This finding is supported by the fact that the human ApoC3-K58E mutation located in the lipid binding domain of ApoC3 results in a marked reduction of triglycerides and VLDLs in plasma (32). Because ApoC3 concentration in the plasma of *Arfrp1*$^{liv-/-}$ mice was markedly reduced but accumulated in the hepatocytes, we hypothesized that ARFRP1 and its downstream effectors are needed for an

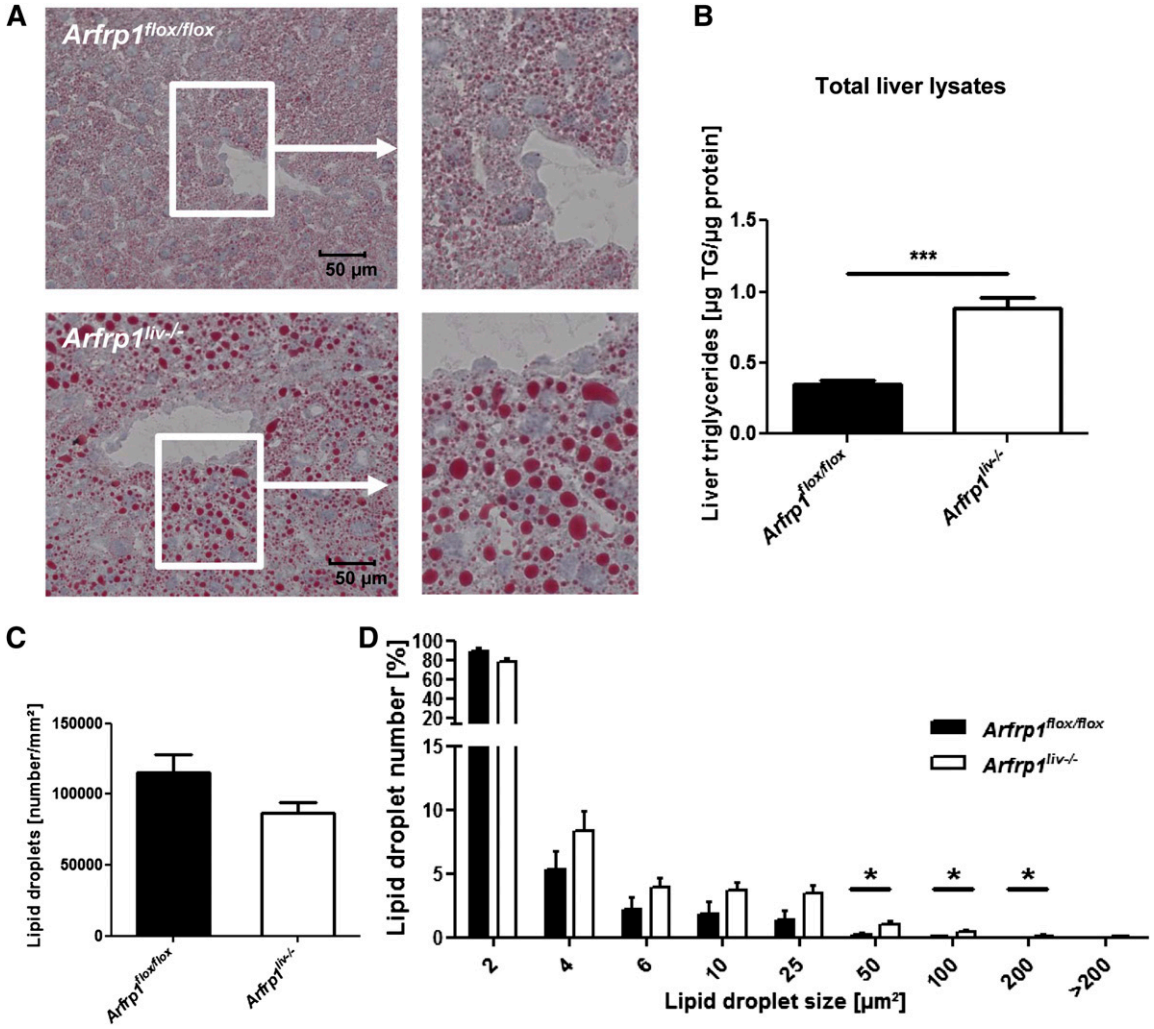

Fig. 6. Elevated hepatic triglyceride storage and altered lipid droplet size in *Arfrp1*$^{liv-/-}$ liver after fasting. Oil-Red O staining of liver cryo sections of *Arfrp1*$^{liv-/-}$ and control mice (A) and analysis of hepatic lipid content (B) indicates an elevated storage in *Arfrp1*$^{liv-/-}$ livers. Quantification of lipid droplet number (C) reveals no significant differences between genotypes. Investigation of lipid droplet sizes (D) in livers of *Arfrp1*$^{liv-/-}$ and control mice. Data are expressed as percentage of lipid droplets in categories of µm^2 (n = 9–11 for liver triglycerides, n = 6 for lipid droplet distribution). *$P < 0.05$, ***$P < 0.001$.

appropriate sorting of ApoC3 to the lumenal lipid droplets that are utilized as a lipid precursor for VLDL assembly. Furthermore, it was already shown by Asp et al. (33) that the Golgi-associated GTPase ARF1, which is involved in retrograde Golgi to ER and intra-Golgi trafficking, is required for final lipidation of VLDL2 particles to form mature lipid-rich VLDL particles (also designated as VLDL1), indicating the important role of the Golgi apparatus for MTP-independent lipid transfer. Furthermore, the deletion of sortilin, an intracellular sorting receptor for ApoB48/100 which is located at the *trans*-Golgi, resulted in a reduced secretion of ApoB48/100 (34). These studies further support the assumption that the *trans*-Golgi compartment is essential for hepatic lipoprotein metabolism. The elevated plasma ApoB48/100 in *Arfrp1*$^{liv-/-}$ mice indicated on the one side that the general release of ApoB48/100-containing particles from *Arfrp1*$^{liv-/-}$ livers is possible. On the other side, these particles, which each carry one ApoB48/100 molecule, carry less triglyceride load. Therefore, the increase in plasma ApoB48/100 appears to be due to the smaller size of VLDL particles. This is also reflected by a lower triglyceride concentration of the HDL-containing fraction that might rather be a contamination with smaller VLDL particles because it is enriched with ApoB48/100 (as shown in Fig. 1E). However, we cannot exclude that the accumulation of ApoB48/100 is the result of an impaired hepatic clearance of VLDL remnants or LDL remnants which could be due to an impaired receptor targeting to the plasma membrane in *Arfrp1*$^{liv-/-}$ hepatocytes based on an altered protein trafficking through the Golgi. Thus, we assume that the triglyceride secretion by *Arfrp1*$^{liv-/-}$ livers is impaired according to two alterations: *1*) by a limited lipidation of VLDL in the Golgi; and *2*) by an impaired ApoC3 release. The overall defect is visible in the fasted state, in which the triglyceride concentration of *Arfrp1*$^{liv-/-}$ mice was reduced by 45%. This effect was smaller (30%) under conditions that blocked the effect of ApoC3 on LPL activity.

The release of limited lipidated VLDLs in *Arfrp1*$^{liv-/-}$ mice secondarily resulted in an accumulation of triglycerides

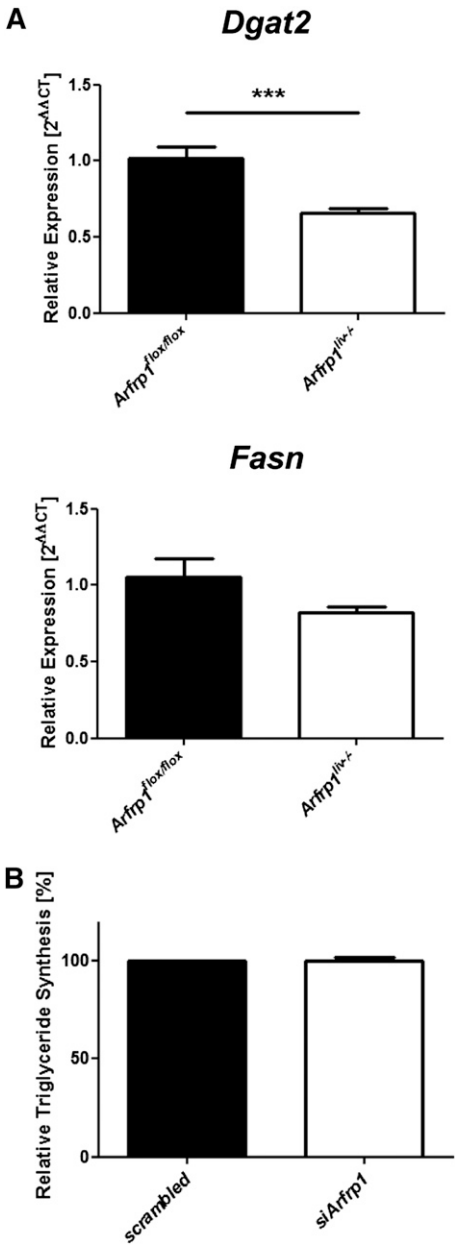

Fig. 7. Unaffected triglyceride synthesis in *Arfrp1*$^{liv-/-}$ hepatocytes. A: Minor changes in expression of enzymes involved in lipid metabolism in *Arfrp1*$^{liv-/-}$ mice. Quantitative real-time PCR of *Fasn* and *Dgat2* mRNA levels in *Arfrp1*$^{liv-/-}$ livers. B: Triglyceride synthesis measured in primary hepatocytes after transfection with scrambled RNA or *siArfrp1* was unaffected. ***$P < 0.001$.

and of ApoB48/100 and ApoC3 under fasting conditions, indicating that ARFRP1 is needed not only for an appropriate lipidation of VLDL particles but also for their release into the plasma. In the absence of ARFRP1, the transport of VLDL particles through the Golgi does not work properly. This was shown by an accumulation of ApoB48/100 and triglycerides in the Golgi (Fig. 4). We currently cannot explain why the levels of ApoB48 in the intracellular fractions are much higher than those of ApoB100, an effect that is also visible in total liver homogenates, while the ratio of both proteins was about equal in plasma samples. Differences in *Apob* mRNA editing induced by prolonged fasting periods could be one explanation. Former studies in rats have demonstrated that thyroid hormone treatment (35) resulted in reduced ApoB100 synthesis. Furthermore, a prolonged fasting period (48 h) and a subsequent high carbohydrate diet resulted in complete loss of ApoB100, which was accounted for by an increase in the proportion of edited *Apob* mRNA (36). The accumulation of triglycerides in the liver of *Arfrp1*$^{liv-/-}$ mice appears to be accompanied by elevated levels of PLIN2, most likely a secondary effect. However, higher expression of PLIN2 in hepatic cell lines inhibits the secretion of VLDL1 (37) and could therefore also influence VLDL lipidation in *Arfrp1*$^{liv-/-}$ mice. The lack of ARFRP1 does not modulate triglyceride synthesis because in vitro triglyceride formation in isolated hepatocytes was not affected after suppression of *Arfrp1* (Fig. 7B). The *Dgat2* mRNA was significantly lower in livers from *Arfrp1*$^{liv-/-}$ mice, indicating that the reesterification of triglycerides could be compensatory, suppressed most likely due to elevated accumulation of triglycerides in these livers (Fig. 6). Another possible explanation for reduced *Dgat2* mRNA is its regulation by low levels of plasma glucose and fasting (38). In fed *Arfrp1*$^{liv-/-}$ mice, blood glucose levels are significantly lower in comparison to control mice (11) and could therefore be causal. Besides VLDL lipidation and therefore hepatic triglyceride release, fasting plasma triglyceride concentrations were further influenced by peripheral clearance mediated by lipoprotein lipase. ApoC3 is a negative regulator of lipoprotein lipase activity (24). Therefore, the reduced levels of ApoC3 in *Arfrp1*$^{liv-/-}$ plasma could lead to a higher activity of lipoprotein lipase which further amplifies the lowering of plasma triglycerides in fasted *Arfrp1*$^{liv-/-}$ mice (Fig. 3).

Another phenotype visible in *Arfrp1*$^{liv-/-}$ mice is the reduced ApoA1 concentration in the plasma. ApoA1 that is synthesized by the liver (and to a lesser extent by the intestine) is the major HDL protein, and both tissues play prime roles in mediating reverse cholesterol transport, the transfer of cholesterol from peripheral tissues, such as arterial wall cells, to the liver for excretion (39, 40). The impaired release of ApoA1 in the absence of ARFRP1 might be responsible for the slightly reduced cholesterol concentration in the total plasma and in the HDL-containing fraction of fasted mice.

Besides the liver, the intestine is the other tissue that produces circulating triglyceride-carrying lipoproteins (41). In a recent study, we showed that chylomicron formation, lipidation as well as apolipoprotein assembly, is dependent on the *trans*-Golgi and ARFRP1 (13). ARFRP1 is required for the correct recruitment and action of other GTPases (ARL1 and Rab proteins) that interact with the scaffolding protein golgin-245. Suppression of each transcript (ARFRP1, ARL1, Golgin-245, Rab2) in Caco-2 cells resulted in a marked reduction of chylomicron release. Thus, it can be speculated that impaired structural capacities at the *trans*-Golgi are responsible for the limited lipidation and maturation of not only chylomicrons, but also of VLDL and HDL particles. The comparison of the phenotype of the intestine-specific with the liver-specific *Arfrp1* knockout identifies strong parallels regarding lipid and lipoprotein metabolism.

In both mouse models the release of ApoB48/100-containing triglyceride-rich particles is impaired and results in lower plasma triglyceride levels and elevated plasma ApoB48/100. In addition, the release of ApoA1 is impaired leading to reduced cholesterol concentration in the plasma of knockout mice. Therefore, the lipidation and the assembly of lipoproteins with apolipoproteins is dependent on ARFRP1 actions at the *trans*-Golgi, a pathway that appears to be conserved in the liver and intestine.

The authors are grateful to Dr. Mark Magnusson, Center for Stem Cell Biology, Vanderbilt University Medical Center, Nashville, TN for providing the alb-Cre. The skillful technical assistance of Monika Niehaus, Andrea Teichmann, and Sarah Ernst is gratefully acknowledged. We thank Prof. Dr. Dr. Hans-Georg Joost for helpful comments and discussions.

REFERENCES

1. Nordestgaard, B. G., M. Benn, P. Schnohr, and A. Tybjaerg-Hansen. 2007. Nonfasting triglycerides and risk of myocardial infarction, ischemic heart disease, and death in men and women. *JAMA.* **298:** 299–308.
2. Bansal, S., J. E. Buring, N. Rifai, S. Mora, F. M. Sacks, and P. M. Ridker. 2007. Fasting compared with nonfasting triglycerides and risk of cardiovascular events in women. *JAMA.* **298:** 309–316.
3. Choi, S. H., and H. N. Ginsberg. 2011. Increased very low density lipoprotein (VLDL) secretion, hepatic steatosis, and insulin resistance. *Trends Endocrinol. Metab.* **22:** 353–363.
4. Sundaram, M., and Z. Yao. 2010. Recent progress in understanding protein and lipid factors affecting hepatic VLDL assembly and secretion. *Nutr. Metab. (Lond.).* **7:** 35.
5. Hesse, D., A. Jaschke, B. Chung, and A. Schurmann. 2013. Trans-Golgi proteins participate in the control of lipid droplet and chylomicron formation. *Biosci. Rep.* **33:** 1–9.
6. Colicelli, J. 2004. Human RAS superfamily proteins and related GTPases. *Sci. STKE.* **2004:** RE13.
7. Wennerberg, K., K. L. Rossman, and C. J. Der. 2005. The Ras superfamily at a glance. *J. Cell Sci.* **118:** 843–846.
8. Zahn, C., A. Hommel, L. Lu, W. Hong, D. J. Walther, S. Florian, H. G. Joost, and A. Schürmann. 2006. Knockout of Arfrp1 leads to disruption of ARF-like1 (ARL1) targeting to the trans-Golgi in mouse embryos and HeLa cells. *Mol. Membr. Biol.* **23:** 475–485.
9. Zahn, C., A. Jaschke, J. Weiske, A. Hommel, D. Hesse, R. Augustin, L. Lu, W. Hong, S. Florian, A. Scheepers, et al. 2008. ADP-ribosylation factor-like GTPase ARFRP1 is required for trans-Golgi to plasma membrane trafficking of E-cadherin. *J. Biol. Chem.* **283:** 27179–27188.
10. Hesse, D., A. Hommel, A. Jaschke, M. Moser, U. Bernhardt, C. Zahn, R. Kluge, P. Wittschen, A. D. Gruber, H. Al-Hasani, et al. 2010. Altered GLUT4 trafficking in adipocytes in the absence of the GTPase Arfrp1. *Biochem. Biophys. Res. Commun.* **394:** 896–903.
11. Hesse, D., A. Jaschke, T. Kanzleiter, N. Witte, R. Augustin, A. Hommel, G. P. Puschel, K. J. Petzke, H. G. Joost, M. Schupp, et al. 2012. GTPase ARFRP1 is essential for normal hepatic glycogen storage and insulin-like growth factor 1 secretion. *Mol. Cell. Biol.* **32:** 4363–4374.
12. Hommel, A., D. Hesse, W. Volker, A. Jaschke, M. Moser, T. Engel, M. Bluher, C. Zahn, A. Chadt, K. Ruschke, et al. 2010. The ARF-like GTPase ARFRP1 is essential for lipid droplet growth and is involved in the regulation of lipolysis. *Mol. Cell. Biol.* **30:** 1231–1242.
13. Jaschke, A., B. Chung, D. Hesse, R. Kluge, C. Zahn, M. Moser, K. J. Petzke, R. Brigelius-Flohe, D. Puchkov, H. Koepsell, et al. 2012. The GTPase ARFRP1 controls the lipidation of chylomicrons in the Golgi of the intestinal epithelium. *Hum. Mol. Genet.* **21:** 3128–3142.
14. Schulz, N., H. Himmelbauer, M. Rath, M. van Weeghel, S. Houten, W. Kulik, K. Suhre, S. Scherneck, H. Vogel, R. Kluge, et al. 2011. Role of medium- and short-chain L-3-hydroxyacyl-CoA dehydrogenase in the regulation of body weight and thermogenesis. *Endocrinology.* **152:** 4641–4651.
15. Lubura, M., D. Hesse, N. Neumann, S. Scherneck, P. Wiedmer, and A. Schurmann. 2012. Non-invasive quantification of white and brown adipose tissues and liver fat content by computed tomography in mice. *PLoS ONE.* **7:** e37026.
16. Molica, F., F. Burger, A. Thomas, C. Staub, A. Tailleux, B. Staels, G. Pelli, A. Zimmer, B. Cravatt, C. M. Matter, et al. 2013. Endogenous cannabinoid receptor CB1 activation promotes vascular smooth-muscle cell proliferation and neointima formation. *J. Lipid Res.* **54:** 1360–1368.
17. Brunham, L. R., J. K. Kruit, J. Iqbal, C. Fievet, J. M. Timmins, T. D. Pape, B. A. Coburn, N. Bissada, B. Staels, A. K. Groen, et al. 2006. Intestinal ABCA1 directly contributes to HDL biogenesis in vivo. *J. Clin. Invest.* **116:** 1052–1062.
18. Peters, J. M., N. Hennuyer, B. Staels, J. C. Fruchart, C. Fievet, F. J. Gonzalez, and J. Auwerx. 1997. Alterations in lipoprotein metabolism in peroxisome proliferator-activated receptor alpha-deficient mice. *J. Biol. Chem.* **272:** 27307–27312.
19. Chen, Z., R. L. Fitzgerald, G. Li, N. O. Davidson, and G. Schonfeld. 2004. Hepatic secretion of apoB-100 is impaired in hypobetalipoproteinemic mice with an apoB-38.9-specifying allele. *J. Lipid Res.* **45:** 155–163.
20. Henkel, J., K. Frede, N. Schanze, H. Vogel, A. Schurmann, A. Spruss, I. Bergheim, and G. P. Puschel. 2012. Stimulation of fat accumulation in hepatocytes by PGE(2)-dependent repression of hepatic lipolysis, beta-oxidation and VLDL-synthesis. *Lab. Invest.* **92:** 1597–1606.
21. Brunham, L. R., R. R. Singaraja, M. Duong, J. M. Timmins, C. Fievet, N. Bissada, M. H. Kang, A. Samra, J. C. Fruchart, B. McManus, et al. 2009. Tissue-specific roles of ABCA1 influence susceptibility to atherosclerosis. *Arterioscler. Thromb. Vasc. Biol.* **29:** 548–554.
22. Graham, J. M., J. A. Higgins, T. Gillott, T. Taylor, J. Wilkinson, T. Ford, and D. Billington. 1996. A novel method for the rapid separation of plasma lipoproteins using self-generating gradients of iodixanol. *Atherosclerosis.* **124:** 125–135.
23. Talmud, P. J., E. Hawe, S. Martin, M. Olivier, G. J. Miller, E. M. Rubin, L. A. Pennacchio, and S. E. Humphries. 2002. Relative contribution of variation within the APOC3/A4/A5 gene cluster in determining plasma triglycerides. *Hum. Mol. Genet.* **11:** 3039–3046.
24. Jong, M. C., P. C. Rensen, V. E. Dahlmans, H. van der Boom, T. J. van Berkel, and L. M. Havekes. 2001. Apolipoprotein C–III deficiency accelerates triglyceride hydrolysis by lipoprotein lipase in wild-type and apoE knockout mice. *J. Lipid Res.* **42:** 1578–1585.
25. Januzzi, J. L., N. Azrolan, A. O'Connell, K. Aalto-Setala, and J. L. Breslow. 1992. Characterization of the mouse apolipoprotein Apoa-1/Apoc-3 gene locus: genomic, mRNA, and protein sequences with comparisons to other species. *Genomics.* **14:** 1081–1088.
26. Yen, C. L., S. J. Stone, S. Koliwad, C. Harris, and R. V. Farese, Jr. 2008. Thematic review series: glycerolipids. DGAT enzymes and triacylglycerol biosynthesis. *J. Lipid Res.* **49:** 2283–2301.
27. Menendez, J. A., A. Vazquez-Martin, F. J. Ortega, and J. M. Fernandez-Real. 2009. Fatty acid synthase: association with insulin resistance, type 2 diabetes, and cancer. *Clin. Chem.* **55:** 425–438.
28. Hussain, M. M., J. Shi, and P. Dreizen. 2003. Microsomal triglyceride transfer protein and its role in apoB-lipoprotein assembly. *J. Lipid Res.* **44:** 22–32.
29. Quiroga, A. D., L. Li, M. Trotzmuller, R. Nelson, S. D. Proctor, H. Kofeler, and R. Lehner. 2012. Deficiency of carboxylesterase 1/esterase-x results in obesity, hepatic steatosis, and hyperlipidemia. *Hepatology.* **56:** 2188–2198.
30. Rustaeus, S., P. Stillemark, K. Lindberg, D. Gordon, and S. O. Olofsson. 1998. The microsomal triglyceride transfer protein catalyzes the post-translational assembly of apolipoprotein B-100 very low density lipoprotein in McA-RH7777 cells. *J. Biol. Chem.* **273:** 5196–5203.
31. Qin, W., M. Sundaram, Y. Wang, H. Zhou, S. Zhong, C. C. Chang, S. Manhas, E. F. Yao, R. J. Parks, P. J. McFie, et al. 2011. Missense mutation in APOC3 within the C-terminal lipid binding domain of human ApoC-III results in impaired assembly and secretion of triacylglycerol-rich very low density lipoproteins: evidence that ApoC-III plays a major role in the formation of lipid precursors within the microsomal lumen. *J. Biol. Chem.* **286:** 27769–27780.
32. von Eckardstein, A., H. Holz, M. Sandkamp, W. Weng, H. Funke, and G. Assmann. 1991. Apolipoprotein C-III(Lys58—Glu). Identification of an apolipoprotein C-III variant in a family with hyperalphalipoproteinemia. *J. Clin. Invest.* **87:** 1724–1731.

33. Asp, L., B. Magnusson, M. Rutberg, L. Li, J. Boren, and S. O. Olofsson. 2005. Role of ADP ribosylation factor 1 in the assembly and secretion of ApoB-100-containing lipoproteins. *Arterioscler. Thromb. Vasc. Biol.* **25:** 566–570.
34. Kjolby, M., O. M. Andersen, T. Breiderhoff, A. W. Fjorback, K. M. Pedersen, P. Madsen, P. Jansen, J. Heeren, T. E. Willnow, and A. Nykjaer. 2010. Sort1, encoded by the cardiovascular risk locus 1p13.3, is a regulator of hepatic lipoprotein export. *Cell Metab.* **12:** 213–223.
35. Davidson, N. O., L. M. Powell, S. C. Wallis, and J. Scott. 1988. Thyroid hormone modulates the introduction of a stop codon in rat liver apolipoprotein B messenger RNA. *J. Biol. Chem.* **263:** 13482–13485.
36. Baum, C. L., B. B. Teng, and N. O. Davidson. 1990. Apolipoprotein B messenger RNA editing in the rat liver. Modulation by fasting and refeeding a high carbohydrate diet. *J. Biol. Chem.* **265:** 19263–19270.
37. Magnusson, B., L. Asp, P. Bostrom, M. Ruiz, P. Stillemark-Billton, D. Linden, J. Boren, and S. O. Olofsson. 2006. Adipocyte differentiation-related protein promotes fatty acid storage in cytosolic triglycerides and inhibits secretion of very low-density lipoproteins. *Arterioscler. Thromb. Vasc. Biol.* **26:** 1566–1571.
38. Meegalla, R. L., J. T. Billheimer, and D. Cheng. 2002. Concerted elevation of acyl-coenzyme A:diacylglycerol acyltransferase (DGAT) activity through independent stimulation of mRNA expression of DGAT1 and DGAT2 by carbohydrate and insulin. *Biochem. Biophys. Res. Commun.* **298:** 317–323.
39. Tall, A. R. 2008. Cholesterol efflux pathways and other potential mechanisms involved in the athero-protective effect of high density lipoproteins. *J. Intern. Med.* **263:** 256–273.
40. Feig, J. E., R. Shamir, and E. A. Fisher. 2008. Atheroprotective effects of HDL: beyond reverse cholesterol transport. *Curr. Drug Targets.* **9:** 196–203.
41. Hegele, R. A. 2009. Plasma lipoproteins: genetic influences and clinical implications. *Nat. Rev. Genet.* **10:** 109–121.